

**Radial focusing of electron wave packets using linearly chirped intense pulses**

M. A. Bouchene

*Laboratoire de Collisions Agrégats Réactivité, CNRS UMR 5589, IRSAMC, Université Paul Sabatier, 118 Route de Narbonne, 31062 Toulouse Cedex 4, France*

(Received 13 December 2002; published 1 August 2003)

We present a theoretical study of the properties of an electron wave packet created by a linearly chirped pulse in the strong-field regime. Radial focusing of the wave packet at macroscopic distances which occurs in the case of a weak laser pulse is still possible but at different time and position. Two different situations are reported. (1) The case of a weakly chirped pulse, for which power broadening of the energy distribution occurs. The electron wave packet focuses to less than the inverse of the pulse spectrum bandwidth. (2) The case of highly chirped pulses, for which a new regime is highlighted where power narrowing of the energy distribution occurs. Saturation effects are shown in this case to improve the quality of focusing by reducing the temporal distortions of the wave packet at the focus point.

DOI: 10.1103/PhysRevA.68.023401

PACS number(s): 42.50.Hz, 32.80.Wr, 32.80.Rm, 32.80.Fb

**I. INTRODUCTION**

The use of ultrashort pulses represents a powerful approach to perform quantum control of both physical and chemical processes [1–3]. One important reason is the possibility to manipulate the spectrum of such pulses in order to design tailored laser pulses for coherent control [4,5]. As an alternative to using fully shaped pulses, significant and spectacular effects can be obtained by simply using chirped pulses. For instance, efficient population transfer via adiabatic following [6], vibrationnal ladder climbing [7], or pump-dump process [8] has been achieved. Wilson *et al.* have shown that negatively chirped pulses can be used to compensate partially for the anharmonicity in the vibrational states, allowing the wave packet to focus at a certain internuclear distance [9,10]. Of special interest here, the case of an electron wave packet created in the continuum. We have shown in a previous paper [11] that positively linearly chirped pulses can be used to manipulate the radial motion of an electron wave packet. The wave packet is then shaped in such a way that it focuses radially at macroscopic distances from the ion core. This has also been reported in the study of the dynamics of autoionizing wave packets in calcium [12]. This effect is interesting since it may open the possibility to design an ultrashort electron pulse source at low energy. The compensation of radial dispersion at the range of centimeters represents an important step to overcome for practical use of ultrashort electron pulses. However, other problems, such as angular focusing and compensation of the spatial dispersion effects, have to be surmounted before performing such a design. When accelerating electrons to high energy with an extracting static field, the spreading becomes negligible. This is the case of ultrafast electron diffraction [13] or high-energy electron diffraction RHEED [14].

The dynamics of electron wave packet have been intensively explored in the case of Rydberg states of one-electron systems. Depending on the nature of excited states, the wave packet can be initially localized radially or angularly [15,16]. Motion of the wave packet is quasiclassical at short times, but at longer times the discrete nature of the spectrum and anharmonicity of the potential lead to quantum

spreading and revivals of the wave packet. Extension to the case of two-electron atoms leads to new effects such as ionization suppression [17], laser induced autoionization [18], and inner electron ionization [19,20]. Calculations have also been performed to design tailored pulses for optimal control of Rydberg electron wave packet dynamics [21], whereas temporal coherent control of energy and angular distribution have been experimentally realized [22].

In our approach, in Ref. [11], we have considered only the weak-field regime. The study of the strong-field regime is a natural extension as a higher level of signal is expected. Moreover, in this regime, the quantum system can have its properties radically changed, leading to new effects where the usual pictures derived from the perturbative approach break down. The saturation of a continuum with a strong laser pulse is a well-known phenomenon (see Ref. [23], and references therein). Moreover, when the continuum presents no resonance, the slowly varying continuum approximation is generally used, allowing a significant simplification of the formalism. Irreversible evolution to the continuum and power broadening of the energy distribution are the most striking consequences of the interaction. For higher intensities, more complex phenomena appear, such as ATI (above threshold ionization) and tunnel ionization.

In this paper, we study the radial focusing of an electron wave packet created by a strong linearly chirped pulse that ionizes an alkali atom. We consider the case where the slowly varying continuum approximation can be done and the intensities considered here are below those required for ATI and tunnel ionization [24,25]. We show that power broadening no longer occurs for highly chirped pulses and the energy distribution turns out to be narrowed with increasing the laser intensity. We study also the changes that occur to the shape of the wave packet near the focus point. Saturation effects are shown for highly chirped pulses to improve the quality of focusing by reducing the distortions that may occur in the weak-field regime, whereas for weakly chirped pulses the wave packet duration is reduced.

**II. THEORETICAL MODEL**

We consider an alkali atom with a single active electron on the outer shell. The system is initially in a bound state

$|\varphi_0\rangle$  and a linearly chirped laser pulse ionizes the atom, thus bringing the electron into the continuum. The continuum states are well described by a simple model where the electron is assumed to be scattered by the ion core represented by a central potential [26,27]. We neglect in this formalism the continuum-continuum coupling and the spin orbit-coupling in the continuum which is known to have a small effect except when the Cooper minimum region is considered [28,29]. In this case, hydrogenlike wave functions  $|\varepsilon, l, m\rangle$  can be used to represent the continuum states ( $\varepsilon$  represents the electron kinetic energy). They are expressed as  $R_{\varepsilon l}(r)Y_{lm}(\theta, \varphi)$  in the  $\vec{r}$  representation [with  $(r, \theta, \varphi)$  representing spherical coordinates of  $\vec{r}$ ]. The distances  $r$  and kinetic energies considered here ( $r > 1 \mu\text{m}$ ,  $\varepsilon > 0.1 \text{ eV}$ ) are high enough to neglect the potential energy when compared to the electron kinetic energy. In this case, we can use an asymptotic expression of the radial function  $R_{\varepsilon l}(r) \simeq_{r \rightarrow \infty} (1/kr) \sin(kr - l\pi/2 + \delta_{\varepsilon l})$ . In this expression,  $\varepsilon = \hbar^2 k^2 / 2m_e$  and  $\delta_{\varepsilon l}$  is the phase shift of the wave function due to the interaction with the central potential. The wave function in the ionization continuum can be written as

$$|\psi(t)\rangle = \sum_{l,m} \int a_{\varepsilon lm}(\varepsilon, t) \exp\left(-i \frac{(\varepsilon + \varepsilon_i)}{\hbar} t\right) |\varepsilon lm\rangle d\varepsilon \quad (1)$$

with the amplitude of transition per square energy unit  $a_{\varepsilon lm}$  given by

$$a_{\varepsilon lm}(\varepsilon, t) = \frac{1}{i\hbar} \int_{-\infty}^t \mu_{\varepsilon lm} E(t') a_0(t') \exp\left(i \frac{(\varepsilon + \varepsilon_i)}{\hbar} t'\right) dt' \quad (2)$$

Here,  $\mu_{\varepsilon lm}$  is the dipole moment between the initial state  $|\varphi_0\rangle$  and the one-electron state  $|\varepsilon lm\rangle$  in the continuum,  $\varepsilon_i$  is the ionization potential from the initial level,  $E(t)$  is the electric field, and  $a_0(t)$  is the amplitude of probability for the initial state. The expression of the wave function in the  $\vec{r}$  representation is obtained by using the asymptotic expression for the radial wave function. We retain only the outward part that corresponds to the emission of an electron. We obtain the following relation:

$$\begin{aligned} \psi(\vec{r}, t) &= \frac{\hbar}{2ikr} \sum_{l,m} Y_m^l(\theta, \varphi) e^{-il\pi/2} \\ &\times \int_{\varepsilon_i/\hbar}^{+\infty} a_{\varepsilon lm}(\omega, t) e^{i(kr + \delta_{\varepsilon l} - \omega t)} d\omega \quad (3) \end{aligned}$$

with  $\omega = (\varepsilon + \varepsilon_i)/\hbar$ . All the properties of the electron wave packet are contained in this equation. The radial and angular motions are linked through the phase shift  $\delta_{\varepsilon l}$ . The spectral dependence of this term is very weak over the laser spectral range and it can in most cases be dropped out of the integral. It plays a role only for very low kinetic energies of the electron ( $\leq 0.1 \text{ eV}$ ), below the range of energy considered here ( $\simeq \text{eV}$ ). The radial and angular parts of the wave function can be factored out [11]. This leads to a time-independent angular distribution that is always delocalized and the wave

packet propagation that is only radial. The problem is reduced to the case of wave packet spreading in one dimension.

The chirped pulse is generally obtained by sending an initial Fourier transform limited pulse in a dispersive medium or apparatus (pair of gratings or prisms, pulse shaper), which induces a quadratic phase shift  $\phi(\omega) \simeq \phi_0''/2(\omega - \omega_L)^2$ . In this expression,  $\omega_L$  is the laser frequency and  $\phi_0''$  represents the amount of chirp introduced. Assuming an initial Fourier-limited Gaussian pulse with an amplitude proportional to  $e^{-(t/\tau_0)^2}$ , the electric field of the pulse  $E(t)$  can be written as

$$E(t) = E_0 \exp\left[-\left(\frac{t}{\tau}\right)^2\right] e^{-i\delta t^2} e^{-i\omega_L t} \quad (4)$$

with

$$\tau = \tau_0 \sqrt{1 + 4 \frac{\phi_0''^2}{\tau_0^4}} \quad (5a)$$

and

$$\delta = \frac{2\phi_0''}{\tau_0^4(1 + 4\phi_0''^2/\tau_0^4)} \quad (5b)$$

Here,  $\tau$  is the duration of the chirped pulse which is broader than the initial pulse and  $\delta$  characterizes the frequency sweeping in time. More precisely, the instantaneous frequency is  $\omega_L + 2\delta t$  and sweeps linearly with a rate characterized by  $\delta$ . The Fourier transform  $\tilde{E}(\omega) = \int_{-\infty}^{+\infty} E(t') e^{i\omega t'} dt'$  that characterizes the field spectrum can be written as

$$\tilde{E}(\omega) \propto e^{-\tau_0^2(\omega - \omega_L)^2/4} e^{i(\phi_0''/2)(\omega - \omega_L)^2} \quad (6)$$

For highly chirped pulses such as  $\phi_0'' \gg \tau_0^2$ , the quadratic phase oscillates strongly. Using the stationary phase approximation, we found that at time  $t$  only the frequency components located in a restricted interval of the order of  $4\sqrt{\pi/\phi_0''}$  around the instantaneous frequency  $\omega_L + 2\delta t$  ( $\delta \simeq 1/2\phi_0''$ ) contribute to the chirped pulse field. From Eq. (5a), we see that  $\tau \simeq 2\phi_0''/\tau_0$ : the chirped pulse behaves as a quasimonochromatic field whose frequency sweeps during the time  $\tau$  from the low-frequency part of the spectrum  $\omega_L - \tau_0^{-1}$  to the high component one  $\omega_L + \tau_0^{-1}$ . This image of the chirped pulse will be useful in the following to highlight the physics of its interaction with the atomic system.

The radial focusing, which occurs when weak laser chirped pulses are used, has been established and discussed in a previous paper [11]. We summarize the main features in the following section and then tackle the case of saturation regime (Sec. IV).

### III. RADIAL FOCUSING OF ELECTRON WAVE PACKET IN THE WEAK-FIELD REGIME

For a positively chirped pulse, radial focusing of an electron wave packet is possible. This can be understood as follows. When  $\phi_0'' > 0$ , the instantaneous frequency is swept

from low frequency ( $< \omega_L$ ) to high frequency ( $> \omega_L$ ) as time increases. In a classical image, the slow electrons are created first and the fast ones will catch up. When the sign of the chirp is reversed, fast electrons are created first and so the delay with the slow electrons increases during the propagation. Obviously, focusing is impossible in this case. We establish in the following the conditions to fulfill in order to get an optimized electron pulse at the focus point.

In the weak-field regime, the initial state is weakly depleted, then  $a_0(t) \approx 1$ . When the ionization process ended ( $t \gg \tau$ ), the amplitude transition expresses as

$$a_{\varepsilon lm}(\omega, t \gg \tau) = \frac{\mu_{\varepsilon lm}}{i\hbar} \tilde{E}(\omega). \quad (7)$$

The energy distribution of the electron reproduces only the pulse spectrum. Using this expression in Eq. (3), the density of electrons,  $N(r, t) \propto |\psi|^2$ , ejected in the continuum for times  $t \gg \tau$  can be written as follows:

$$N(r, t) \propto \left| \int e^{-\tau_0^2(\omega - \omega_L)^2/4} e^{i[kr + \phi_0''(\omega - \omega_L)^2/2 - \omega t]} d\omega \right|^2. \quad (8)$$

For unchirped pulses,  $\phi_0'' = 0$ . The electron wave packet spreads in the vacuum because of the nonlinear dependence of the free motion phase  $kr$  with the energy. When the electron energy distribution is smaller than the mean kinetic energy  $\bar{\varepsilon} = \hbar(\omega_L - \omega_I)$ , we have

$$\tau_0^{-1} \ll \bar{\varepsilon}/\hbar. \quad (9)$$

In this case, the free phase  $\sigma(r, t, \omega) = kr - \omega t$  can be expanded as a function of  $\omega$  around  $\omega_L$ :

$$\begin{aligned} \sigma(r, t, \omega) \approx & [k(\omega_L)r - \omega_L t] + \left( r \sqrt{\frac{m}{2\hbar(\omega_L - \omega_I)}} - t \right) \Delta\omega \\ & - \left( r \sqrt{\frac{m}{32\hbar(\omega_L - \omega_I)^3}} \right) (\Delta\omega)^2 \\ & + \left( r \sqrt{\frac{m}{2\hbar(\omega_L - \omega_I)^5}} \right) \frac{(\Delta\omega)^3}{8} + \dots \end{aligned} \quad (10)$$

The first-order term is responsible for the translation of the electron wave packet. In the stationary phase approximation, the most important contribution arises from values of  $(r, t)$  which cancel this term. This leads to the well-known relation  $r = v_g t$ , with  $v_g = [2\hbar(\omega_L - \omega_I)/m]^{1/2}$  the group velocity: the maximum of the wave packet moves at a constant speed and behaves classically. Higher-order terms contribute to the spreading of the wave packet that broadens with time in the radial direction.

When  $\phi_0'' \neq 0$ , the chirp introduces a quadratic phase that cancels the second-order term in Eq. (10) for a position  $r_f$  given by

$$r_f = \sqrt{\frac{8}{m\hbar^2}} \phi_0'' \bar{\varepsilon}^{3/2}. \quad (11)$$

The broadening of the electronic pulse is now determined by the contribution of the third-order term to the phase in Eq. (10). This contribution is negligible only if this term is  $\ll 2\pi$ , which can be written as

$$\left( \frac{\pi}{\hbar} \right) \frac{\bar{\varepsilon} \tau_0^3}{\phi_0''} \gg 1. \quad (12)$$

When this condition is realized, the electron density at  $r = r_f$  is given by  $N(r_f, t) \propto e^{-2(t - r_f/v_g)^2/\tau_0^2}$ . Moreover, the wave packet represents the inverse Fourier transform of the amplitude  $a_{\varepsilon lm}$ . Its temporal behavior reproduces the laser-pulse profile, and perfect focusing of the wave packet is then achieved at the position  $r_f$ . Beyond this position, the wave packet spreads again in the same manner as it spreads after its creation near the ion core. The quantum spreading cannot be suppressed in free space for all positions. The focusing time  $t_f = r_f/v_g$ , from Eq. (11), is

$$t_f = \frac{2\phi_0'' \bar{\varepsilon}}{\hbar}. \quad (13)$$

Focusing occurs really only if time  $t_f$  verifies  $t_f \gg \tau$  to ensure that the wave packet is entirely emitted in time when it reaches the focusing point. This condition was needed to use the expression of the laser-pulse spectrum in Eqs. (7) and (8). The strong limitation to the focusing comes from condition (12) that needs higher kinetic energy for the electron and moderate chirping for the pulse. The strong dependence on the pulse duration makes the focusing for very short pulses difficult. When relation (12) is not fulfilled, the wave packet exhibits oscillations in the wings which are a signature of third-order contributions, similar to those observed in the temporal profile of ultrashort pulses when odd-order contributions cannot be compensated.

The order of magnitude for  $r_f$  lies in the centimeter range for large values of the chirp parameter. For instance, in the case of potassium ( $V_{ion} = 4.28$  eV), if the system is initially prepared in the  $4p$  state, with an ionization wavelength  $\lambda = 339$  nm, the kinetic energy of the electron is  $\bar{\varepsilon} = 2$  eV. For  $\phi_0'' = 2 \times 10^7$  fs<sup>2</sup>, the focusing distance is as large as 10.95 cm and we have  $t_f = 127$  ns which is larger than  $\tau$ , even if pulses as short as 400 fs are used (for which  $\tau \approx 0.1$  ns). For these values, we have  $(\pi/\hbar) \bar{\varepsilon} \tau_0^3 / \phi_0'' \approx 31$  and thus inequality (12) is verified. If the initial pulse was unchirped, the time duration of the electron pulse at the focus point would be equal to  $\tau$ . The compression rate in this case is  $\tau/\tau_0 = 250$ . An efficient focusing is thus obtained. This effect is shown in Fig. 1 where we represent the electron density near the focus point in the time-space representation.

#### IV. SATURATION REGIME

When the strength of the laser pulse is increased, the initial state is substantially depleted. The approximation  $a_0 \approx 1$  does not hold in this case and relation (7) is no longer valid. The value of  $a_0$  can be easily determined in the case where the continuum is structureless, which allows the use of the slow variation continuum approximation and the adiabatic elimination of the continuum. This is the case of alka-

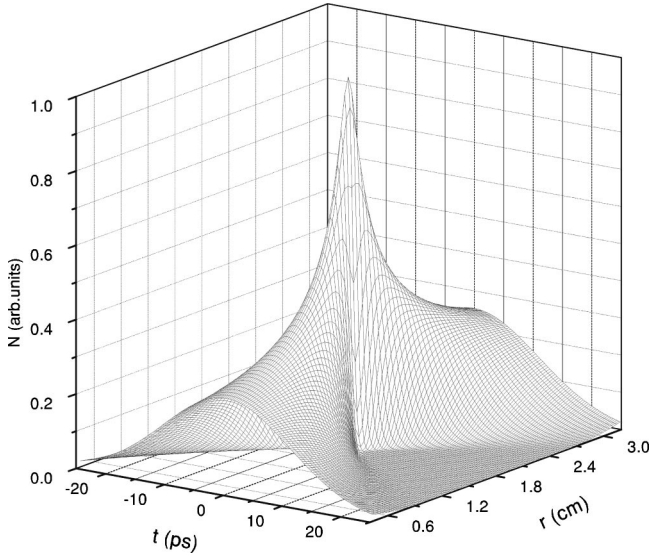


FIG. 1. Focusing of the electronic wave packet in the  $(r,t)$  representation.  $N(r,t)$  is the electronic density represented for  $\tau_0 = 1$  ps,  $\phi_0'' = 10^7$  fs, and  $\bar{\varepsilon} = 1$  eV. A time translation  $t \rightarrow t - r/v_g$  has been performed to make the density centered around time zero.

line metals, where in the energy range of interest there is no autoionizing state that can lead to the presence of resonances. An analytical expression can then be derived for the initial-state amplitude that decreases exponentially in our case as (see, for instance, Refs. [30,31]).

$$a_0(t) = \exp\left[-\int_{-\infty}^t \frac{\Gamma(t')}{2} dt'\right] \quad (14)$$

with the ionization rate  $\Gamma$  given by

$$\Gamma(t) = \frac{2\pi\bar{\mu}^2}{\hbar} |E(t)|^2 \quad (15)$$

with  $\bar{\mu}^2 = \sum_{l,m} \mu_{\varepsilon lm}^2$ , the summation is over all the electron states that can be excited from the initial state. The ionization rate depends on the pulse intensity rather than on the field amplitude. The initial-state amplitude at the end of the pulse involves the time-integrated ionizing rate and hence depends on the energy radiance (in  $\text{J}/\text{m}^2$ ) of the exciting pulse. Except for losses that might be introduced by the chirping apparatus, the chirping of a pulse does not change the energy contained in the pulse. The saturation regime is thus obtained for the same energy radiance of the chirped or unchirped pulse. The decrease of the intensity when chirping the pulse is compensated by the increase of the time duration of the pulse from  $\tau_0$  to  $\tau$  according to formula (5a). An order of magnitude can be given for the energy radiance needed to reach saturation. In the case of potassium prepared initially in the  $4p P_{3/2}$  state,  $S_{1/2}$  and  $D_{3/2,5/2}$  orbitals can be excited in the continuum with a one-photon transition. For a linearly polarized laser field with  $\lambda = 335$  nm, we obtain  $\bar{\mu}^2 = 14.07$  a.u. and the saturation regime ( $\int_{-\infty}^+ \Gamma(t) dt = 1$ ) is reached for  $I\tau = 28$   $\text{mJ}/\text{cm}^2$ , where  $I = 2c\varepsilon_0 |E_0|^2$  is the peak laser intensity and  $\tau$  is the time duration. For an initial pulse with  $\tau_0 = 1$  ps, the required intensity is  $2.8 \times 10^{10}$   $\text{W}/\text{cm}^2$ . If the

chirp parameter is  $\phi_0'' = 10^7$   $\text{fs}^2$ , it gives  $\tau \approx 20$  ps and the peak laser intensity  $I$  of the chirped pulse is then only  $1.4 \times 10^9$   $\text{W}/\text{cm}^2$ . These values are far from the intensity required to observe ATI transitions ( $\geq 10^{12}$   $\text{W}/\text{cm}^2$ ) and justify the negligence of continuum-continuum transitions in our model.

The change in the expression of the initial-state amplitude has a great impact on the behavior of the transition amplitudes  $a_{\varepsilon lm}$  and the electron wave packet. Moreover, the energy distribution of the electrons is no longer representative of the laser-pulse spectrum. We show in Sec. IV A that the interaction with the strong chirped pulse can be described in terms of an effective weak field allowing us to use the results obtained in Sec. III. Then we focus in Sec. IV B on the behavior of the transition amplitudes and the new energy distribution. Finally, we study in Secs. IV C and IV D the new behavior of the electron wave packet, especially at the focus point.

### A. Description in terms of effective weak field

The amplitude of the transition  $a_{\varepsilon lm}$  is expressed from Eqs. (2) and (14) as

$$a_{\varepsilon lm}(\varepsilon, t) = \frac{1}{i\hbar} \int_{-\infty}^t \mu_{\varepsilon lm} E_{eff}(t') \exp\left[i \frac{(\varepsilon + \varepsilon_I)}{\hbar} t'\right] dt' \quad (16)$$

with

$$E_{eff}(t) = E(t) \exp\left[-\int_{-\infty}^t \frac{\Gamma(t')}{2} dt'\right]. \quad (17)$$

These expressions suggest that compared to the weak-field regime where  $E_{eff} = E$ , the effect of the strong field consists in changing the expression of the interacting field from  $E$  to  $E_{eff}$ . An important feature is that only the envelope is affected by this transformation, since  $\Gamma$  is real. This analogy is very convenient for understanding the behavior of the electron wave packet under the strong field, since its properties in the case of weak-field regime have already been determined. This analogy will represent the key idea through this paper to understand the changes in the dynamics of atomic systems in the strong-field regime. We examine now the shape of the envelope of the effective weak field which contains all the information due to the strong field. For the Gaussian given in relation (4), an analytical expression for the effective field can be found. From the relation  $\int_{-\infty}^{-x} e^{-x'^2} dx' = (\sqrt{\pi}/2) \text{erfc}(x)$  where  $\text{erfc}$  is the complementary error function, the following expression for  $E_{eff}$  may be derived:

$$E_{eff}(t) = E_0 f(t) e^{-i\delta t^2} e^{-i\omega_L t}, \quad (18)$$

where

$$f(t) = e^{-(t/\tau)^2} \exp\left[-\frac{s}{4} \text{erfc}(-\sqrt{2}t/\tau)\right] \quad (19)$$

is the envelope of the effective weak field,  $s = [(\pi)^{3/2}/\sqrt{2}] \bar{\mu}^2 / c\varepsilon_0 \hbar I \tau$  is a parameter that characterizes the saturation and depends on the energy radiance  $I\tau$ . An

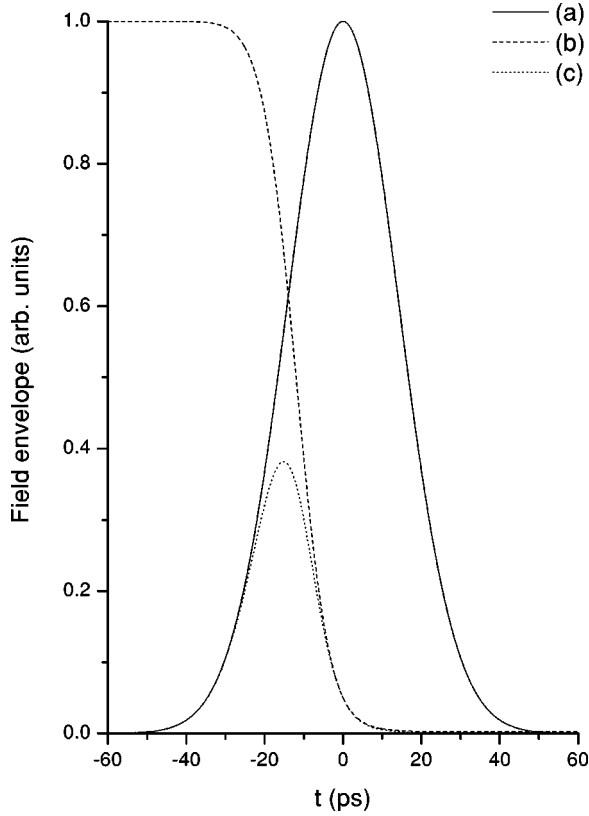


FIG. 2. (a) Field envelope of the chirped pulse  $e^{-(t/\tau)^2}$  that ionizes the atom, (b) amplitude of the initial level  $e^{-(s/4)\text{erfc}(-\sqrt{2}t/\tau)}$ , (c) envelope of the effective weak field  $f(t) = e^{-(t/\tau)^2} e^{-(s/4)\text{erfc}(-\sqrt{2}t/\tau)}$ . The laser parameters here are  $\tau_0 = 1$  ps,  $\phi_0'' = 10^7$  fs<sup>2</sup>, and so  $\tau \approx 20$  ps. The saturation parameter is  $s = 12$ .

example of the time dependence of the different envelopes above is shown in Fig. 2. We report the envelope of the chirped pulse  $e^{-(t/\tau)^2}$  [curve (a)], the amplitude of the initial level  $e^{-(s/4)\text{erfc}(-\sqrt{2}t/\tau)}$  for  $s = 12$  [curve (b)], and the resulting effective weak-field envelope  $f(t)$  [curve (c)] which is the product of the two terms. For the chosen value of the saturation parameter, the initial level is depleted well before the pulse ended. The interaction time between the laser pulse and the atomic system is thus reduced, and the system is sensitive to only a small part of the laser pulse located on its rising edge. The effective weak field turns to be time shifted, and its time duration reduced. Another effect is the decrease in the maximum of the envelope when the laser intensity increases. However, for the amplitudes  $a_{\epsilon lm}$  given in Eq. (16), this effect is counterbalanced by the contribution of  $E_0$  to the effective field (18) that increases and the population in the continuum as well. This result is consistent with the conservation law of population that states that the population in the excited state at the end of the interaction time is  $\sum_{l,m} \int |a_{\epsilon lm}|^2 d\epsilon = 1 - |a_0|^2 = 1 - e^{-s}$  and so increases and saturates after with  $s$ .

We represent in Fig. 3 the variation of the time shift  $\tau_{shift}$  and the temporal width of the effective field  $\tau_{eff}$  as a function of the saturation parameter. These quantities expressed in units of  $\tau$  depend exclusively on  $s$ . The definition of the

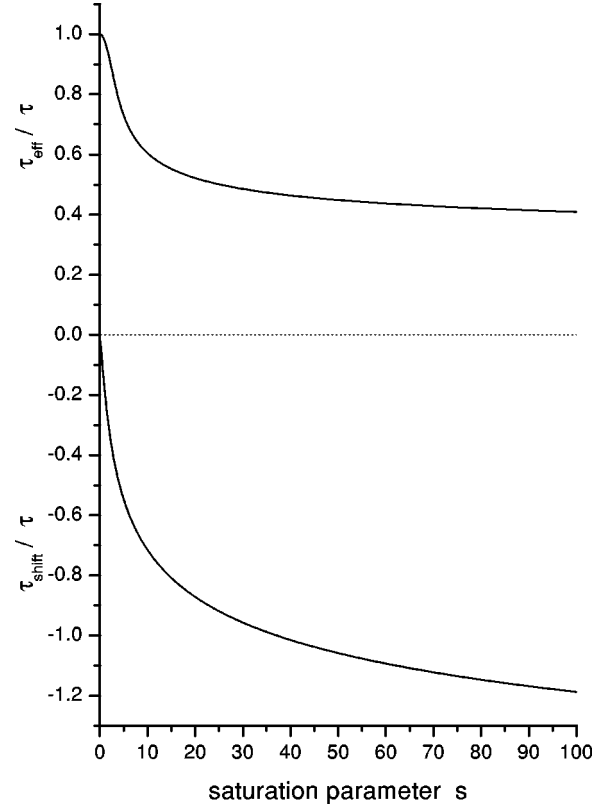


FIG. 3. Variation of the time shift  $\tau_{shift}$  and the temporal width of the effective field  $\tau_{eff}$  as a function of the saturation parameter  $s$ .  $\tau_{shift}$  and  $\tau_{eff}$  are expressed in units of  $\tau$ .

temporal width is the half width at  $1/e$  of the maximum. This definition is convenient in our case because it gives  $\tau_{eff} = \tau$  exactly in the weak-field regime. Moreover, the effective weak field can be well fitted by a Gaussian envelope for the range of intensity saturation considered here, which will allow us, in the next paragraphs, to approximate many quantities with analytical expressions thus highlighting the physics of the interaction. Exact numerical simulations are performed each time to confirm the results obtained with this approach. Two quantities  $\tau_{shift}$  and  $\tau_{eff}$  decrease rapidly with  $s$  until  $s \approx 10$  and vary slowly thereafter. For large values of the saturation parameter such as  $s \gg \sqrt{8\pi}$ , an analytical expression can be found for the time shift  $\tau_{shift} \approx -\tau(\ln \sqrt{s/\sqrt{8\pi}})^{1/2}$  that turns out to be of the same order of magnitude as the chirped pulse duration  $\tau$ . For the duration of the effective field, no analytical expression is possible. For large values of  $s$ , the time duration is reduced more than 40% of its value  $\tau$  in the weak-field regime. In the following, we discuss the consequences that the previous features induce on the transitions amplitudes.

## B. Energy distribution of the electrons: Power broadening and power narrowing

In the weak-field regime, from relation (7) the amplitudes  $a_{\epsilon lm}(t)$  are proportional to the laser field spectrum for  $t \gg \tau$ . In our case, the same relation holds but with the effective weak field introduced above. The energy distribution in

the continuum thus exhibits the properties of the spectrum of this effective field. Using relations (16)–(19), we obtain the following expression:

$$a_{\varepsilon lm}(\omega, t \gg \tau) = \frac{\mu_{\varepsilon lm}}{i\hbar} \tilde{E}_{eff}(\omega), \quad (20)$$

where

$$\begin{aligned} \tilde{E}_{eff}(\omega) = & E_0 e^{i(\omega - \omega_L)\tau_{shift}} e^{-i\delta\tau_{shift}^2} \int_{-\infty}^{+\infty} f_c(t') \\ & \times e^{-i\delta t'^2} e^{i(\omega - \omega_L - 2\delta\tau_{shift})t'} dt' \end{aligned} \quad (21)$$

is the spectrum of the effective field (18) and  $f_c(t) = f(t + \tau_{shift})$  represents the envelope of the effective field centred around  $t = 0$ .

For unchirped pulses,  $\delta = 0$ . The comparison between the saturation regime and the case of weak-field regime for which  $\tau_{shift} = 0$  and  $f_c(t) = e^{-(t/\tau_0)^2}$  shows that the expression of the transition amplitudes differs by a phase factor  $e^{i(\omega - \omega_L)\tau_{shift}}$  and the expression of the envelope  $f_c$ . The phase factor reflects the effect of the time shift induced by the strong field on the spectrum and does not affect the energy distribution of the electrons. However, the shape of the envelope is changed because of the shortening of the time duration of the effective field in the saturation regime. As a result, the electron energy distribution which involves the Fourier transform of the effective field envelope spreads over a spectral domain of the order of  $2\tau_{eff}^{-1}$ , and so is larger than the pulse spectrum width  $2\tau_0^{-1}$  (half width at  $1/e$  of the maximum). This is the well-known phenomenon of power broadening in the continuum.

For chirped pulses,  $\delta \neq 0$ . The time shift introduces a contribution to the phase integral in relation (21) which is equivalent to a change in the central laser frequency from  $\omega_L$  to  $\omega_L + 2\delta\tau_{shift}$ . This effect can be explained from the definition (4) for the chirped pulses. The instantaneous frequency is  $\omega_L + 2\delta t$  and sweeps linearly with time  $t$ . The translation by  $\tau_{shift}$ , which occurs for the effective field, induces automatically a frequency shift of  $2\delta\tau_{shift}$ . Thus, the energy distribution of the electrons is no longer centered around the kinetic energy  $\bar{\varepsilon}$ . Note that this change is due to the combined effects of chirp and saturation, for which both  $\delta$  and  $\tau_{shift}$  are not vanishing. From relation (5b) and the behavior of  $\tau_{shift}$  which depends on the chirp through only the value of  $\tau$ , we find that this shift increases with the chirp parameter  $\phi_0''$  and saturates for highly chirped pulses such as  $\phi_0'' \gg \tau_0^2$ . It reaches then a maximum value whose analytical expression is  $(2/\tau_0)(\ln \sqrt{s/\sqrt{8\pi}})^{1/2}$  for  $s \gg \sqrt{8\pi}$ .

The energy distribution of the electrons around the shifted central frequency  $\omega_L + 2\delta\tau_{shift}$  depends on the behavior of the term  $f_c(t)e^{-i\delta t^2}$  in the integral of expression (21). For chirp values such as  $\delta\tau_{eff}^2 \leq 1$ , where  $\tau_{eff}$  is the time duration of the effective envelope, the quadratic phase term above introduces small changes and power broadening is still expected. However, for large values of the chirp such as  $\delta\tau_{eff}^2 \gg 1$ , the phase term oscillates strongly and significant changes follow. Using the stationary phase approximation in

this case, we find that the nonvanishing amplitudes  $a_{\varepsilon lm}$  are those associated with frequencies located in an interval of the order of  $2\delta\tau_{eff}$  around the shifted central frequency  $\omega_L + 2\delta\tau_{shift}$  [the same result can be obtained by performing an analytical integration of the integral in Eq. (21) with a Gaussian approximation for the envelope  $f_c$ ]. Remembering that  $\tau$  and  $\tau_{eff}$  are of the same order of magnitude [see Fig. 3], and from relations (5a) and (5b), the inequality  $\delta\tau_{eff}^2 \gg 1$  is equivalent to  $\phi_0'' \gg \tau_0^2$ . It follows that  $\delta \approx 1/2\phi_0''$ ,  $\tau \approx 2\phi_0''/\tau_0$  and thus the energy distribution spreads out over a spectral domain of the order of  $2\tau_0^{-1}(\tau_{eff}/\tau)$  smaller than the laser spectrum width  $2\tau_0^{-1}$ . In contrast with the cases of Fourier-transform-limited pulses or weakly chirped pulses that lead to power broadening, the case of highly chirped pulses such as  $\phi_0'' \gg \tau_0^2$  leads to power narrowing of the energy distribution of the electrons. This spectacular change may also be explained from the particular properties of the chirped pulse spectrum. As noted in the last part of Sec. II, the chirped pulse behaves as a quasimonochromatic field whose frequency sweeps during the time  $\tau$  from the low-frequency part of the spectrum  $\omega_L - \tau_0^{-1}$  to the high component one  $\omega_L + \tau_0^{-1}$ . The interaction of such a pulse with the atomic system in the saturation regime makes the system feel only a part of the pulse spectrum, because the depletion of the initial state reduces the time interaction from  $\tau$  to  $\tau_{eff}$  around the time shift  $\tau_{shift}$ . The energy distribution of the emitted electrons reflects only the contribution of the frequency components swept during this time. Because the sweep is linear, the concerned spectral domain is  $2\tau_0^{-1}(\tau_{eff}/\tau)$ , and so is smaller than the pulse spectrum width  $2\tau_0^{-1}$ . It also follows from these arguments that the energy distribution is shifted to the low part of the pulse spectrum, which confirms the above result that predicts a shift in the central frequency from  $\omega_L$  to  $\omega_L + 2\delta\tau_{shift}$ . The electron dynamic is then insensitive to the high-frequency components of the pulse spectrum. The power narrowing of the electron spectrum follows the variation of the ratio  $(\tau_{eff}/\tau)$  that decreases slowly when increasing the laser intensity [see Fig. 3]. We represent in Fig. 4 the energy distribution of electrons ( $\propto |\tilde{E}_{eff}|$ ) for the following parameters  $\bar{\varepsilon} = 1$  eV,  $\tau_0 = 500$  fs, and (a)  $\phi_0'' = 0$ ,  $s \approx 0$ ; (b)  $\phi_0'' = 3 \times 10^4$  fs<sup>2</sup>,  $s = 12$ ; (c)  $\phi_0'' = 10^7$  fs<sup>2</sup>,  $s = 12$ . The distributions are normalized to unity to make a clear comparison between the corresponding bandwidths. Note that for such laser intensity, the ionization concerns with nearly 100% ( $1 - e^{-12}$ ) of the total population in the initial level. In case (a), the case of weak-field regime for which the energy distribution does not depend on the chirp parameter and matches exactly the pulse spectrum is represented (bandwidth 2.5 meV at  $1/e$  of the maximum). The distribution is centred around the mean value  $\bar{\varepsilon} = 1$  eV. When saturation is considered, a different behavior occurs. In case (b), the chirp parameter has a non-negligible value, but it is still weak enough ( $\phi_0''/\tau_0^2 = 0.12$ ) to make the quadratic phase of the laser-pulse spectrum vary slowly. As discussed above, power broadening occurs and the energy distribution broadens here to 4.1 meV. In case (c), the chirp parameter is such as  $\phi_0''/\tau_0^2 = 40$ . Here, we are in the

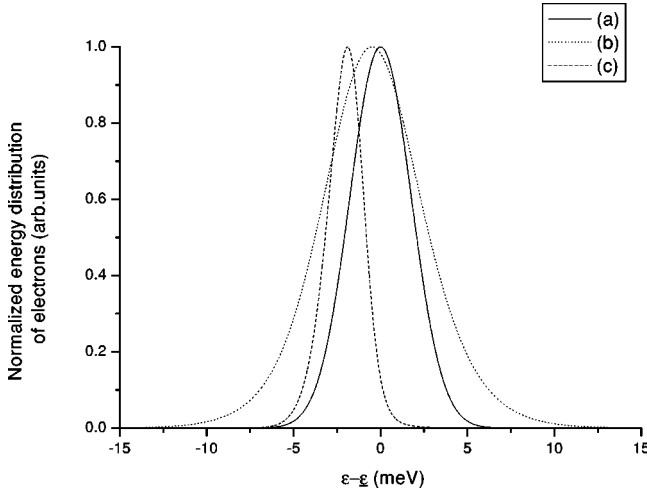


FIG. 4. Energy distribution of the electrons in the continuum ( $\propto |a_{elm}|$ ). Here  $\bar{\varepsilon} = 1$  eV and  $\tau_0 = 500$  fs (duration before chirping). Case (a) corresponds to the situation of the weak-field regime with no chirp, so  $\phi_0'' = 0$ ,  $s = 0$ . Case (b) represents the situation of the strong-field regime with a small amount of chirp ( $\phi_0'' = 3 \times 10^4$  fs<sup>2</sup>,  $s = 12$ ) and case (c) corresponds to the strong-field regime with highly chirped pulses ( $\phi_0'' = 10^7$  fs<sup>2</sup>,  $s = 12$ ). The energy distribution matches the laser field spectrum in (a), whereas (b) and (c) give rise to power broadening and power narrowing, respectively.

case of highly chirped pulses, where the system is sensitive only to the lower part of the laser spectrum. As a result, the energy distribution narrows from 2.5 to 1.42 meV in comparison with the weak-field regime. The maximum of the distribution is also shifted in both cases (b) and (c) by  $-0.51$  and  $-1.9$  meV respectively, in good agreement with the prediction above that gives the analytical estimations  $\delta\bar{\varepsilon} = 2\hbar\delta\tau_{shift}$  for the energy shift [ $= -0.47$  (b),  $= -1.99$  meV (c)],  $2\hbar\tau_{eff}^{-1} (= 4.19$  meV) and  $2\hbar\tau_0^{-1}(\tau_{eff}/\tau) (= 1.44$  meV) for the energy bandwidth in the case of weakly and highly chirped pulses, respectively (the analytical expressions would be rigorously exact if the effective weak-field envelope was a perfect Gaussian).

The changes observed in the amplitude transitions when saturation occurs have significant impact on the temporal evolution of the electron wave packet. In the following section, we discuss the changes that occur for the focusing of the wave packet.

### C. Radial focusing of electron wave packet in the saturation regime: Temporal and spatial shifts

The electron wave packet is connected to the transition amplitude  $a_{elm}$  by relation (3) and depends on the laser spectrum of the effective field. From relations (3), (20), and (21), the electron density can be written as

$$N(r, t) \propto \left| \int |\tilde{E}_{eff}(\omega)| e^{i[kr + \phi_{eff}(\omega) - \omega(t - \tau_{shift})]} d\omega \right|^2, \quad (22)$$

where  $\phi_{eff}(\omega)$  is the phase of the effective field spectrum

whose expression can be approximated by the following analytical expression  $\phi_{eff}(\omega) \approx \phi_0''_{eff}(\omega - \omega_L - 2\delta\tau_{shift})^2/2$ , where  $\phi_0''_{eff} = \phi_0'' + \Delta\phi_0''$  with

$$\Delta\phi_0'' = \phi_0'' \frac{\left(\frac{\tau_{eff}}{\tau}\right)^4 - 1}{1 + \left[\left(\frac{2\phi_0''}{\tau_0^2}\right)^2 \left(\frac{\tau_{eff}}{\tau}\right)^4\right]}. \quad (23)$$

$\Delta\phi_0''$  is the variation of the chirp parameter due to saturation effects and is always negative. This correction vanishes in the weak-field regime for which  $\tau_{eff}/\tau = 1$  or for large values of the chirp parameter such as  $\phi_0'' \rightarrow \infty$ . Important changes are expected in all other cases.

In the weak-field regime,  $\tau_{shift} \approx 0$  and  $|\tilde{E}_{eff}(\omega)| \propto e^{-(\omega - \omega_L)^2 \tau_0^2/4}$ . The wave packet focuses in the radial direction at a distance  $r_f$  given by relation (11), and at time  $t_f$  given by Eq. (13) that depends on the kinetic energy  $\bar{\varepsilon}$  and the chirp parameter  $\phi_0''$ . In the saturation regime, the chirp parameter is modified, the frequency distribution is shifted by  $2\delta\tau_{shift}$ , and the term  $\tau_{shift}$  induces a global time translation of the electron wave packet [see Eq. (22)]. Note that this last effect is present whether the laser pulse is chirped or not, and is due to the fact that in the saturation regime, the rapid depletion of the initial level makes the laser field interact with the atomic system only during the rising edge of the pulse, and as a result the wave packet is time shifted. All these changes make both the focusing distance and the focusing time modified. Because the energy and time shifts are small compared with  $\bar{\varepsilon}$  and  $t_f$ , respectively, the most important contribution comes from the change in the chirp parameter. However, for large values of  $\phi_0''$ ,  $\Delta\phi_0'' \rightarrow 0$ , the corrections due to the energy and time shifts, even if small, cannot be neglected, because, as will be shown next, they can exceed the spatial and temporal extensions of the electron wave packet.

The radial distance of focusing is affected only by the change in the chirp parameter and the mean kinetic energy since it does not involve the time application of the laser. The focusing distance is found from relation (11) to be reduced from  $r_f$  to  $r_{feff} = r_f + \Delta r_f$  with

$$\Delta r_f \approx r_f \left( \frac{\Delta\phi_0''}{\phi_0''} + \frac{3\delta\bar{\varepsilon}}{2\bar{\varepsilon}} + \frac{3\Delta\phi_0''\delta\bar{\varepsilon}}{2\phi_0''\bar{\varepsilon}} \right). \quad (24)$$

For the focusing time, the changes occur because of all of the three shifts cited above. The time shift  $\tau_{shift} (< 0)$  of the effective field advances the creation of the electron wave packet. The lowering of the mean kinetic energy from  $\bar{\varepsilon}$  to  $\bar{\varepsilon} + \delta\bar{\varepsilon}$  decreases both the velocity group  $v_g (\propto \bar{\varepsilon}^{1/2})$  and the focusing distance  $r_f (\propto \bar{\varepsilon}^{3/2})$ . However, even if the wave packet slows down, the stronger energy dependence of  $r_f$  reduces the focusing distance at a larger rate, and the focusing time reduces as a result. Finally, the reducing of the chirp parameter makes also the focusing time lower from  $t_f$  to  $t_f + t_f(\Delta\phi_0''/\phi_0'')$ . The total time delay  $\Delta t_f = t_{feff} - t_f$  of the wave packet is the sum of the contributions of the three effects ( $t_{feff}$  is the modified focusing time). Using expression (13), we find

$$\Delta t_f \approx \tau_{shift} + t_f \left( \frac{\Delta \phi_0''}{\phi_0''} + \frac{\delta \bar{\varepsilon}}{\bar{\varepsilon}} + \frac{\Delta \phi_0'' \delta \bar{\varepsilon}}{\phi_0'' \bar{\varepsilon}} \right). \quad (25)$$

For large values of the chirp such as  $\phi_0'' \rightarrow \infty$ , we have  $\delta \bar{\varepsilon} \approx \hbar \tau_{shift} / \phi_0''$  and  $\Delta \phi_0'' \approx 0$ , so  $\Delta t_f \approx 3 \tau_{shift} (< 0)$ . As noted above, even in this case where only the time and energy shifts give important contributions, the time delay is of the same order of magnitude as the chirped pulse duration  $\tau$ , and so much higher than the temporal width at the focus point, which is around  $\tau_0$ . Some values for the above shifts can be given now. For laser pulses with  $\tau_0 = 1$  ps  $\phi_0'' = 10^7$  fs<sup>2</sup>, and  $s = 12$ , and if  $\bar{\varepsilon} = 1$  eV, we obtain  $\Delta t_f \approx -629.2$  ps and  $\Delta r_f \approx -37$   $\mu$ m with  $t_f \approx 30.36$  ns and  $r_f \approx 1.8$  cm. The shift in the time delay is important but still weak in comparison with the focusing time ( $\Delta t_f / t_f \approx 2\%$ ). For weakly chirped pulses such as  $\phi_0'' = 3 \times 10^4$  fs<sup>2</sup> and the same values for the other parameters, we obtain  $\Delta t_f \approx -81.55$  ps and  $\Delta r_f \approx -47.77$   $\mu$ m which are of the same order of magnitude of  $t_f \approx 91.1$  ps and  $r_f \approx 53.98$   $\mu$ m. The wave packet is then significantly shifted in time and space in this last case.

#### D. Radial focusing of electron wave packet in the saturation regime: Wave packet shape

The shape of the wave packet at the focus point is an important property that inform us on the quality of the focusing obtained with this method. In the weak-field regime (cf. Sec. II), when condition (12) is satisfied, the wave packet turns out to be proportional to the inverse Fourier transform of the transition amplitudes  $a_{\varepsilon lm}$ . The time duration is therefore given by the inverse of the electron distribution which matches exactly the laser spectrum. Hence, the wave packet reproduces the laser-pulse profile before chirping and the focusing is at a maximum.

In the saturation regime, the same features hold but now with the use of the effective weak field whose spectrum bandwidth is different from  $\tau_0^{-1}$ . Depending on the chirp, the effective weak-field spectrum may be larger (power broadening) or smaller (power narrowing) than the initial laser spectrum. The electron wave packet is thus expected to be at the focus point shorter or larger than the initial unchirped pulse, respectively. The expressions for the time duration can be approximated by the analytical values  $\tau_{eff}$  and  $\tau_0(\tau_{eff}/\tau)^{-1}$ , respectively, and these are rigorously valid if the effective weak-field envelope was a perfect Gaussian. We represent in Fig. 5 the result of a numerical estimation of the square root of the electron density ( $\propto |\psi|$ ) at the focus point for the following situations: (a) represents the case of a weak-field regime ( $s \approx 0$ ), (b) the case of saturation for a weakly chirped pulse ( $s = 12$ ,  $\phi_0'' = 3.10^4$  fs<sup>2</sup>), and (c) the case of saturation for a highly chirped pulse ( $s = 12$ ,  $\phi_0'' = 10^7$  fs<sup>2</sup>). The unchirped pulse is such that  $\tau_0 = 500$  fs and the mean kinetic energy is  $\bar{\varepsilon} = 1$  eV. The curves are normalized to 1, to make better comparisons between the different bandwidths, and zero time represents the arrival time of the maximum of the electron wave packet at the focus point. The time duration (defined here as the half width at  $1/e$  of the maximum) is found to be equal to 500, 296, and 840 fs,

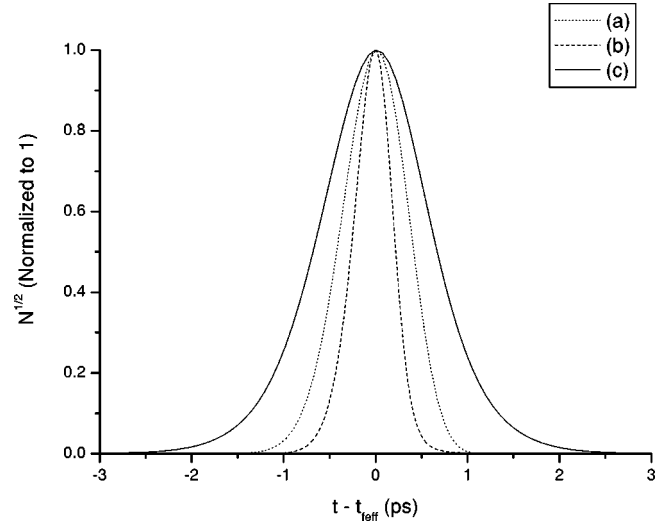


FIG. 5. Temporal profile of the square root of the electron density  $N(r_{eff}, t)$  (normalized to 1) at the focus point for the following situations: (a) weak-field regime ( $s \approx 0$ ), (b) saturation regime with moderately chirped pulses ( $s = 12$ ,  $\phi_0'' = 3 \times 10^4$  fs<sup>2</sup>), and (c) saturation regime with highly chirped pulses ( $s = 12$ ,  $\phi_0'' = 10^7$  fs<sup>2</sup>). The other parameters are  $\tau_0 = 500$  fs and  $\bar{\varepsilon} = 1$  eV.

respectively, whereas the analytical expressions give  $\tau_{eff} \approx 292$  fs and  $\tau_0(\tau_{eff}/\tau)^{-1} \approx 862$  fs. Thus, power broadening leads to the creation of electron pulses significantly shorter than the unchirped laser pulse (by 204 fs). Note that in such a situation, however, the chirp parameter is weak and the focusing distance is small (here, we obtain  $r_{eff} \approx 6.21$   $\mu$ m). In the opposite case of high chirped pulses, the electron pulse focuses at large distances ( $r_{eff} \approx 1.8$  cm), but experiences important time broadening ( $\sim 340$  fs) in comparison with the weak-field regime.

When condition (12) is not satisfied, the electron wave packet can no longer be correctly focused. In the weak-field regime, this inequality represents a strong constraint to the focusing of ultrashort electron pulses for which the spectrum bandwidth  $\tau_0^{-1}$  is large. Due to the third-order contribution in the phase  $\sigma$ , strong temporal oscillations appear in the wave packet profile that is hence distorted [11]. In the saturation regime, the inequality (12) involves the bandwidth of the effective field spectrum instead of  $\tau_0^{-1}$ . For highly chirped pulses such as  $\phi_0'' \gg \tau_0^2$ , power narrowing occurs. Condition (12) is hence less restrictive than in the case of the weak-field regime. Saturation leads in this case to the reduction of the distortion of the wave packet at the focus point. An electron pulse that is distorted in the weak-field regime may be correctly focused on increasing the intensity. This important result is shown in Fig. 6. An initial laser pulse with a Gaussian envelope such as  $\tau_0 = 250$  fs [represented in Fig. 6(a)] is broadened by a dispersive medium with  $\phi_0'' = 10^7$  fs<sup>2</sup>. It ionizes the atomic medium and the mean kinetic energy of ejected electrons is  $\bar{\varepsilon} = 0.5$  eV. In the weak-field regime ( $s \approx 0$ ), the left term in relation (12) is only 3.75 and the third-order contribution cannot be neglected any longer. This is observed in curve (b) which represents the electron pulse profile at the focus point. The wave packet is clearly dis-

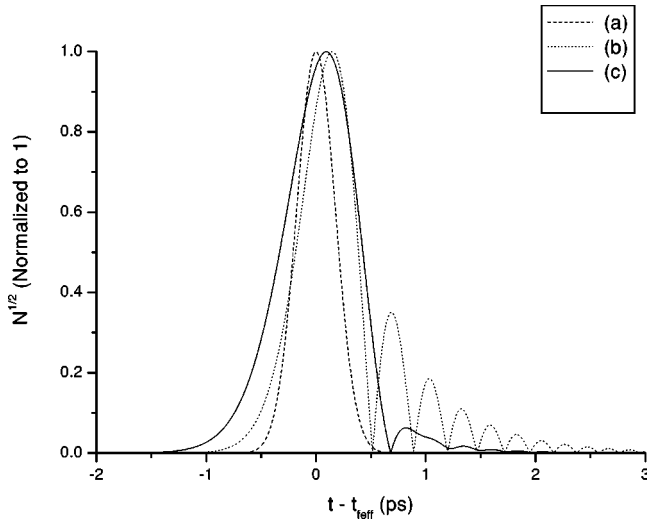


FIG. 6. Temporal profile of the square root of the electronic density  $N(r_{eff}, t)$  (normalized to 1) at the focus point, (b) weak-field regime where  $s=0$ , (c) saturation regime with  $s=12$ . The parameters for both cases are  $\tau_0=250$  fs,  $\phi_0''=10^7$  fs<sup>2</sup>, and  $\bar{\epsilon}=0.5$  eV. Curve (a) represents the pulse envelope of the initial laser pulse  $e^{-(t/\tau_0)^2}$ .

torted and presents strong oscillations in the tail. When the intensity is increased [ $s=12$ , case (c)], a different behavior occurs. Although the wave packet experiences time broadening because of the power narrowing of the spectrum, the oscillations are strongly attenuated thus improving the quality of the electron pulse at the focus. Finally, we consider the case of weakly chirped pulses such as  $\phi_0'' \leq \tau_0^2$ . In this situation, power broadening occurs but the low value of the chirp parameter ensures that the relation (12) is almost always verified. Moreover, in this case, the left term in Eq. (12) is higher than  $5\bar{\epsilon}$  (eV) $\tau_0$  (fs) and is then much greater than one, except for very low kinetic energy and very short pulses. The electron wave packet is thus not affected by high-order contributions to the phase  $\sigma$ , and focuses correctly with a time bandwidth shorter than  $\tau_0$ .

## V. CONCLUSION

We have presented a detailed study of the behavior of electron wave packets created by strong chirped pulses for which the ionization process is almost total. We have shown that radial focusing still occurs in this regime. However, important new features appear. One striking result is the possibility for highly chirped pulses such as  $\phi_0'' \gg \tau_0^2$  to produce energy distributions for the electrons narrower than the pulse spectrum, in complete opposition to the case of Fourier-transform-limited or weakly chirped pulses for which power broadening occurs. These effects modify substantially the shape of the wave packet that is also found to focus at different times and positions. Moreover, when power broadening occurs, the wave packet focuses with a temporal width shorter than the time duration of the ionizing pulse before

chirping, whereas in the case of power narrowing the temporal width is larger. In this last case, the saturation was shown to improve the quality of the focusing substantially, by reducing the distortions that occur in the weak-field regime.

Many effects predicted in this paper can be observed. For instance, power narrowing by a factor between 1 and 2.5 might be observed. For instance, if a chirped pulse with  $\tau_0=50$  fs and  $\phi_0''=10^5$  fs<sup>2</sup> ionizes an atom, the energy distribution of the electrons narrows from 28 meV in the weak-field regime to 17 meV in the saturation regime with  $s=10$ . This can be easily observed with an electron spectrometer of few meV resolution [32]. The observation of time focusing of the electron wave packet represents a more difficult challenge. It depends on the time resolution of the detectors and on the severity of the effect of spatial dispersion of the atoms over the laser spot. However, an experiment under realistic conditions is possible. For instance, with a limited-Fourier-transform pulse  $\tau_0=200$  fs yielding to electron pulses with a kinetic energy of 2 eV, the electron wave packets broaden to 200 ps after 11 cm flight in the vacuum because of spreading. Assuming a laser spot of about 20  $\mu$ m diameter, the spatial dispersion leads to about 25 ps spreading. The measure of electron pulses may be done in a streak camera arrangement that gives a resolution of a few picoseconds or even less [13,33]. Once this laser pulse is chirped to  $\phi_0''=2 \times 10^7$  fs<sup>2</sup>, the electron wave packet focuses at the same distance to the initial laser-pulse duration (200 fs). This cannot be measured, of course, but a reducing of the time broadening of the electron signal can be observed in the detector from 200 ps to a value about 25 ps due to the spatial dispersion.

The prediction of the changes that occur for the electron energy distribution when a chirped strong laser pulse ionizes a system may be important in photoelectron spectroscopy. For instance, if several autoionization channels are present, the resulting dynamics for the electrons depends crucially on the energy distribution of electrons around these resonances. A detailed understanding of this behavior is then crucial to analyze experimental results. Moreover, the results present here apply if a continuum of dissociation is considered instead of the continuum ionization. The translational motion and the inner states of products may be considerably changed when multichannels are involved in a predissociation process. For laser intensities higher than those considered here, other ionization processes such as ATI will come into play. The opening of these new channels may considerably reduce the time interaction between the atomic system and the chirped pulse. Depending on the chirp, one can expect to produce a distribution for the electron energy peaks that is narrower or broader than the laser spectrum.

## ACKNOWLEDGMENTS

We sincerely acknowledge V. Blanchet, J. Vigué, and A. Beswick for stimulating discussions, and C. Marsden for a critical reading of the manuscript.

- [1] H. Rabitz, R. de Vivie-Riedle, M. Motzkus, and K. Kompa, *Science* **288**, 824 (2000).
- [2] M. Shapiro and P. Brumer, *Adv. At., Mol., Opt. Phys.* **42**, 287 (2000).
- [3] S. A. Rice, *Nature (London)* **409**, 422 (2001).
- [4] T. Brixner, N. H. Damrauer, and G. Gerber, *Adv. At., Mol., Opt. Phys.* **46**, 1 (2001).
- [5] A. M. Weiner, *Rev. Sci. Instrum.* **71**(5), 1929 (2000).
- [6] J. S. Melinger, A. Hariharan, S. R. Gandhi, and W. S. Warren, *J. Chem. Phys.* **95**, 2210 (1991).
- [7] D. J. Maas, D. I. Duncan, R. B. Vrijen, W. J. van der Zande, and L. D. Noordam, *Chem. Phys. Lett.* **290**, 75 (1998).
- [8] G. Cerullo, C. J. Bardeen, Q. Wang, and C. V. Shank, *Chem. Phys. Lett.* **262**, 362 (1996).
- [9] B. Kohler, V. V. Yakovlev, J. Che, J. L. Krause, M. Messina, K. R. Wilson, N. Schwentner, R. M. Whitnell, and Y. Yan, *Phys. Rev. Lett.* **74**, 3360 (1995).
- [10] M. Ben-Num, J. Cao, and K. R. Wilson, *Phys. Chem. A* **101**, 8743 (1997).
- [11] J. C. Delagnes and M. A. Bouchene, *J. Phys. B* **35**, 1819 (2002).
- [12] M. Millet, M. Aymar, E. Luc-Koenig, and J. M. Lecomte, *J. Phys. B* **35**, 875 (2002).
- [13] J. C. Williamson, J. Cao, H. Ihee, H. Frey, and A. H. Zewail, *Nature (London)* **386**, 159 (1997).
- [14] H. E. Elsayed-Ali and J. W. Herman, *Rev. Sci. Instrum.* **61**, 1636 (1990).
- [15] J. A. Yeazell and C. R. Stroud, Jr., *Phys. Rev. Lett.* **60**, 1494 (1988); J. A. Yeazell, M. Mallalieu, J. Parker, and C. R. Stroud, Jr., *Phys. Rev. A* **40**, 5040 (1989).
- [16] A. ten Wolde, L. D. Noordam, A. Lagendijk, and H. B. van Linden van den Heuvell, *Phys. Rev. Lett.* **61**, 2099 (1988).
- [17] J. H. Hoogenraad, R. B. Vrijen, and L. D. Noordam, *Phys. Rev. A* **50**, 4133 (1994).
- [18] R. B. Vrijen, J. H. Hoogenraad, and L. D. Noordam, *Phys. Rev. A* **52**, 2279 (1995).
- [19] H. Stapelfeldt, D. G. Papaioannou, L. D. Noordam, and T. F. Gallagher, *Phys. Rev. Lett.* **67**, 3223 (1991).
- [20] R. R. Jones and P. H. Bucksbaum, *Phys. Rev. Lett.* **67**, 3215 (1991).
- [21] J. L. Krause, K. J. Schafer, M. Ben-Nun, and K. R. Wilson, *Phys. Rev. Lett.* **79**, 4978 (1997); L. E. E. de Araujo, I. A. Walmsley, and J. C. R. Stroud, *ibid.* **81**, 955 (1998); L. E. E. de Araujo and I. A. Walmsley, *Phys. Rev. A* **63**, 023401 (2001).
- [22] R. van Leeuwen, M. L. Bajema, and R. R. Jones, *Phys. Rev. Lett.* **82**, 2852 (1999).
- [23] P. L. Knight, M. A. Lauder, and B. J. Dalton, *Phys. Rep.* **190**, 1 (1990).
- [24] R. Marani and E. J. Robinson, *J. Phys. B* **32**, 711 (1999).
- [25] Dong-Gun-Lee, Jung-Hoon-Kim, Kyung-Han-Hong, and Chang-Hee-Nam, *Phys. Rev. Lett.* **87**, 243902 (2001).
- [26] I. I. Sobelman, *Atomic Spectra and Radiative Transitions*, 2nd ed. (Springer, Berlin, 1992).
- [27] M. Aymar, O. Robaux, and S. Wane, *J. Phys. B* **17**, 993 (1984).
- [28] U. Fano, *Phys. Rev.* **178**, 131 (1969).
- [29] P. Lambropoulos, *Phys. Rev. Lett.* **30**, 413 (1973).
- [30] A. G. Abrashkevich and M. Shapiro, *J. Phys. B* **29**, 627 (1996).
- [31] E. Frishman and M. Shapiro, *Phys. Rev. A* **54**, 3310 (1996).
- [32] P. Baltzer, L. Karlsson, M. Lundqvist, and B. Wannberg, *Rev. Sci. Instrum.* **64**, 2179 (1993).
- [33] G. M. Lankhuijzen and L. D. Noordam, *Opt. Commun.* **129**, 361 (1996).